Development of Low-Cost Remote-Control Generators Based on BiTe Thermoelectric Modules

Luis E. Juanicó, Fabián Rinalde, Eduardo Taglialavore & Marcelo Molina

Journal of Electronic Materials

ISSN 0361-5235

Journal of Elec Materi
DOI 10.1007/s11664-012-2431-9

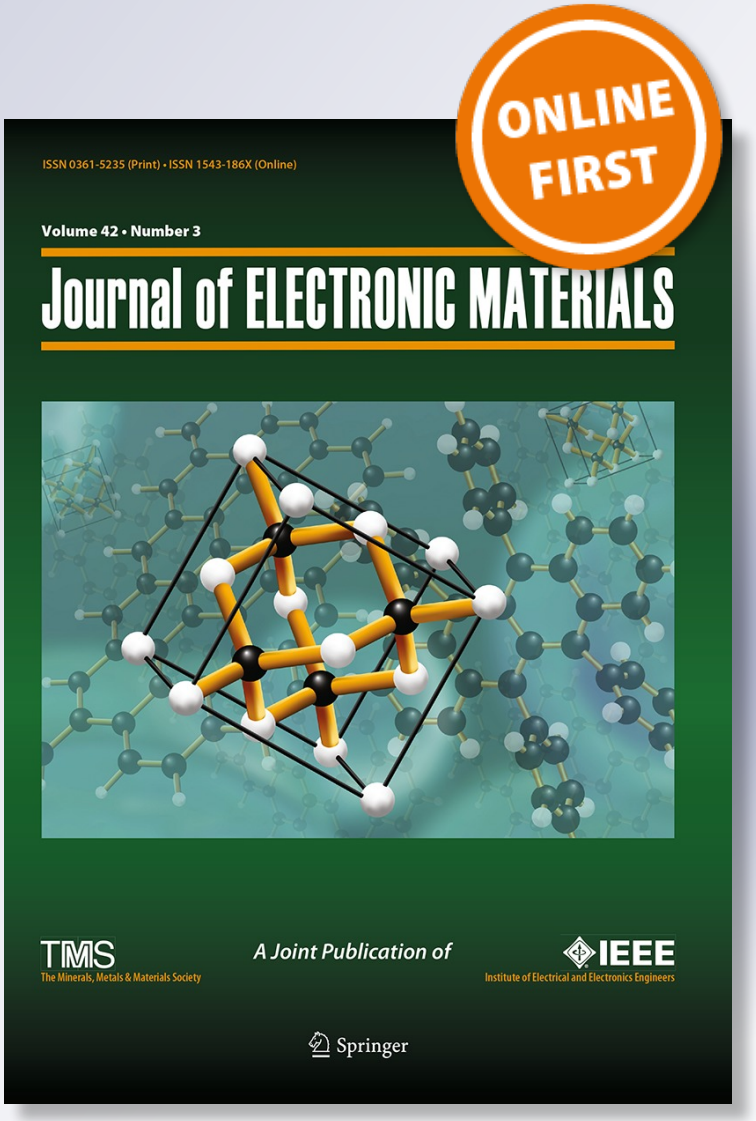

Springer

Your article is protected by copyright and all rights are held exclusively by TMS. This e-offprint is for personal use only and shall not be self-archived in electronic repositories.
If you wish to self-archive your work, please use the accepted author's version for posting to your own website or your institution's repository. You may further deposit the accepted author's version on a funder's repository at a funder's request, provided it is not made publicly available until 12 months after publication.

Author's personal copy

Journal of ELECTRONIC MATERIALS
DOI: 10.1007/s11664-012-2431-9
© 2013 TMS

Development of Low-Cost Remote-Control Generators Based on BiTe Thermoelectric Modules

LUIS E. JUANICÓ,[1,2] FABIÁN RINALDE,[1] EDUARDO TAGLIALAVORE,[1] and MARCELO MOLINA[1]

1.—National Research Council (Conicet) and Balseiro Institute, Bariloche Atomic Center, 8400 Bariloche, Argentina. 2.—e-mail: juanico@cab.cnea.gov.ar

This paper presents a new thermogenerator based on moderate-temperature (up to 175°C) BiTe modules available on the open market. Despite this handicap relative to commercial thermogenerators based on high-temperature proprietary-technology PbBi modules (up to 560°C), this new design may become economically competitive due to its innovative thermal sink. Our thermal sink is based on a free-convection water loop built with standard tubing and household hot-water radiators, leading to a more practical, modular design. So, the specific cost of about 55,000 USD/kW obtained for this 120-W prototype is improved to 33,000 USD/kW for a 1-kW unit, which represents about half the price of commercial thermogenerators. Moreover, considering recently launched BiTe modules (that withstand up to 320°C), our proposition could have an even more favorable outlook.

Key words: BiTe thermoelectric modules, thermoelectricity, thermogenerator, electrical generators, prototype, thermal–hydraulic design

INTRODUCTION

Up to now there is only a single niche market for thermogenerators (TE) (related to powering remote loads for the oil and gas industry) that can afford prices of about 60,000 USD/kW.[1] Since 1975, this market has only been served by Global Thermoelectric, manufacturing thermogenerators based on its high-temperature (up to 560°C) PbBi modules. This kind of proprietary-technology module allows Global Thermoelectric to design a compact cooling system based on a finned dissipator that works at about 130°C.[1] On the other hand, use of BiTe modules working at moderate temperatures (up to 175°C) that are available on the open market implies a major challenge regarding this small temperature drop, in order to develop a new thermogenerator with competitive costs. Recent studies on BiTe prototypes have proposed the use of vacuum closed loops[2] or fan-cooled finned dissipators.[3–5] The former alternative has obtained a modest improvement (120°C) for the cooling system, whereas the latter implies significant self-consumption of energy (more than 50% of the TE's generation) related to the fan.[4,5] Therefore, it is necessary to explore new choices in order to develop a competitive TE based on BiTe technology.

In this paper a new thermogenerator is presented, which was developed to solve the lack of a competitive BiTe thermogenerator. The major innovations relate to: (1) a low-cost passive cooling system that works down to 50°C, and (2) a microcontroller system that manages the heating power to ensure safe operation and the possibility of maximizing the power under any conditions. In this way, new thermogenerators based on cheap BiTe modules, such as Tellurex (4,000 USD/kW)[6] or Thermonamic (2,500 USD/kW), could be obtained.[7] A first 120-W prototype was built and tested, showing that these goals are achievable.

PROTOTYPE DEVELOPMENT

This prototype was built on 16 G1-54-0557 Tellurex modules mounted between two aluminum

(Received June 22, 2012; accepted December 28, 2012)

Published online: 12 February 2013

Author's personal copy

plates, a heating collector, and a dissipator. Both the top side of the collector as well as the bottom side of the dissipator are square in shape (244 mm × 244 mm) and fit the module assembly, whereas the bottom side of the collector is a larger square that fits onto the infrared gas burner and the top side of the dissipator is a large circle (420 mm diameter) that provides a suitable base for the water heat exchanger. This assembly is illustrated in Fig. 1. Here, cylindrical fins that are used to enhance the heat transferred to the water plenum are screwed over the dissipator. From this heat exchanger (shown at the bottom of Fig. 2) the heated water flows upward through the central chimney (a 3-inch-diameter steel pipe) and exits radially through eight low-cost household hot-water radiators (100 USD each). From here the cold flow goes downward through eight 1-inch-diameter tubes back to the water plenum. This closed water loop provides a modular design that can easily be scaled up to higher power. Concerns about water freezing in cold locations could be avoided just by using a standard nonfreezable fluid. The capacity of this fluid mixture to transport heat could be slightly lower than water, but in this case (at lower ambient temperatures) this is not a problem at all. The large chimney and huge surface of dissipation guarantee good thermal–hydraulic performance whereas costs are kept down, as analyzed in the next sections.

THERMAL–HYDRAULIC MODELING

The thermal and hydraulic regimes are coupled in this natural convection flow driven by the buoyancy pressure drop (Δp_b) originating from the difference in density (δ) between the hot and cold legs of the water circuit, known as a "heat pump." This closed loop is illustrated in Fig. 3, where T_i and L_i are the temperature and length of the i-th section, respectively. This cooling circuit transfers the heating power from the thermopile to the environment according to a thermal resistance that ultimately determines its thermal performance, which can be calculated first via the hydraulic model. Although in any free-convection flow the thermal and hydraulic behaviors are coupled, the closed-loop case is rather similar to a forced convection regime because only the heat pump results in a coupling term in the momentum equation. So, the hydraulic regime is characterized here by the dimensionless Reynolds number (that approximates the ratio of inertial forces to viscous forces) rather than the Grashof number (that approximates the ratio of buoyancy forces to viscous forces). Therefore, the flow can be first determined as a function of a given set of cold and hot temperatures. Secondly, these temperatures are calculated from energy balances (in the heat exchanger and the radiators) considering the previous value of the cooling flow, then following an iterative process between the momentum and energy equations to determine the actual values for the cooling flow and all the temperatures.

Δp_b can be calculated by the momentum equation, Eq. 1[8]:

$$\Delta pb(\delta) = -\delta(T_1)L_1 + \delta\left(\frac{T_1+T_2}{2}\right)L_3. \tag{1}$$

This Δp_b is balanced by hydraulic pressure losses due to both distributed (Δp_d) and concentrated (Δp_c) pressure losses. The distributed losses can be calculated by Eq. 2[8]:

$$\Delta p_b(\delta) = \frac{1}{2}f_1(Re_1)\frac{L_1}{D_1}\delta(T_1)V_1^2 + \frac{1}{2}f_2(Re_2)\frac{L_2+L_5}{D_1}\delta(T_2)V_2^2 + \frac{1}{2}f_2(Re_2)\frac{L_4}{D_2}\delta(T_1)V_2^2, \tag{2}$$

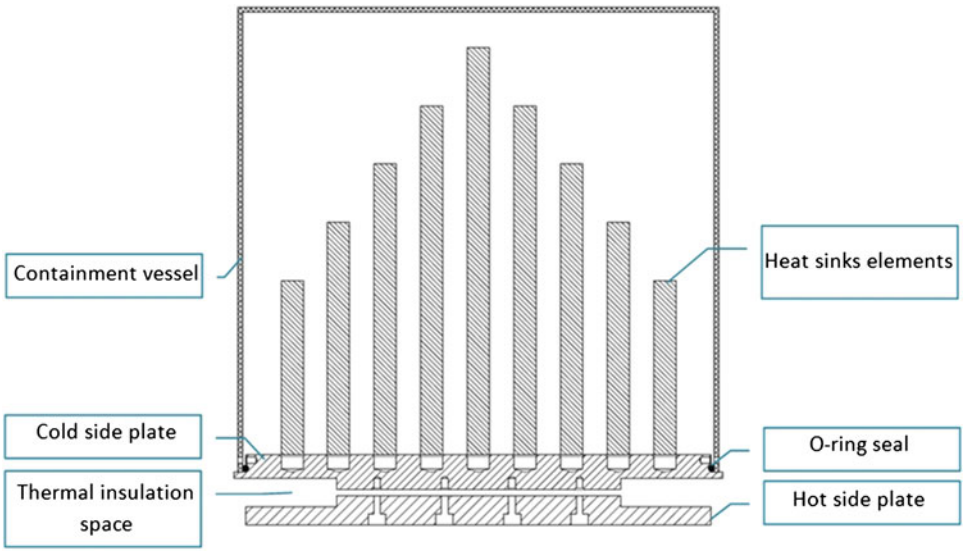

Fig. 1. Schematic of the thermopile assembly.

Author's personal copy

where f_i, D_i, and V_i are the Darcy friction coefficient, hydraulic diameter, and mean velocity in the i-th section, respectively; here f is calculated from its Reynolds number $Re_i = D_i V_i / \nu_i$ (ν being its kinematic viscosity) as Eq. 3[8]:

$$f_i = \frac{64}{Re_i} \quad \text{if } Re < 10,000, \tag{3a}$$

$$f_i = 0.316\, Re_i^{-\frac{1}{4}} \quad \text{if } 10,000 < Re < 20,000, \tag{3b}$$

$$f_i = 0.184\, Re_i^{-\frac{1}{5}} \quad \text{if } Re > 20,000. \tag{3c}$$

Similarly, the concentrated pressure losses can be calculated by Eq. 4[8] as

$$\Delta p_c(\delta) = \frac{1}{2}(K_1 + K_2 + K_6)\delta(T_1)V_1^2 + \frac{1}{2}(K_2 + K_4 + K_5)\delta(T_2)V_2^2. \tag{4}$$

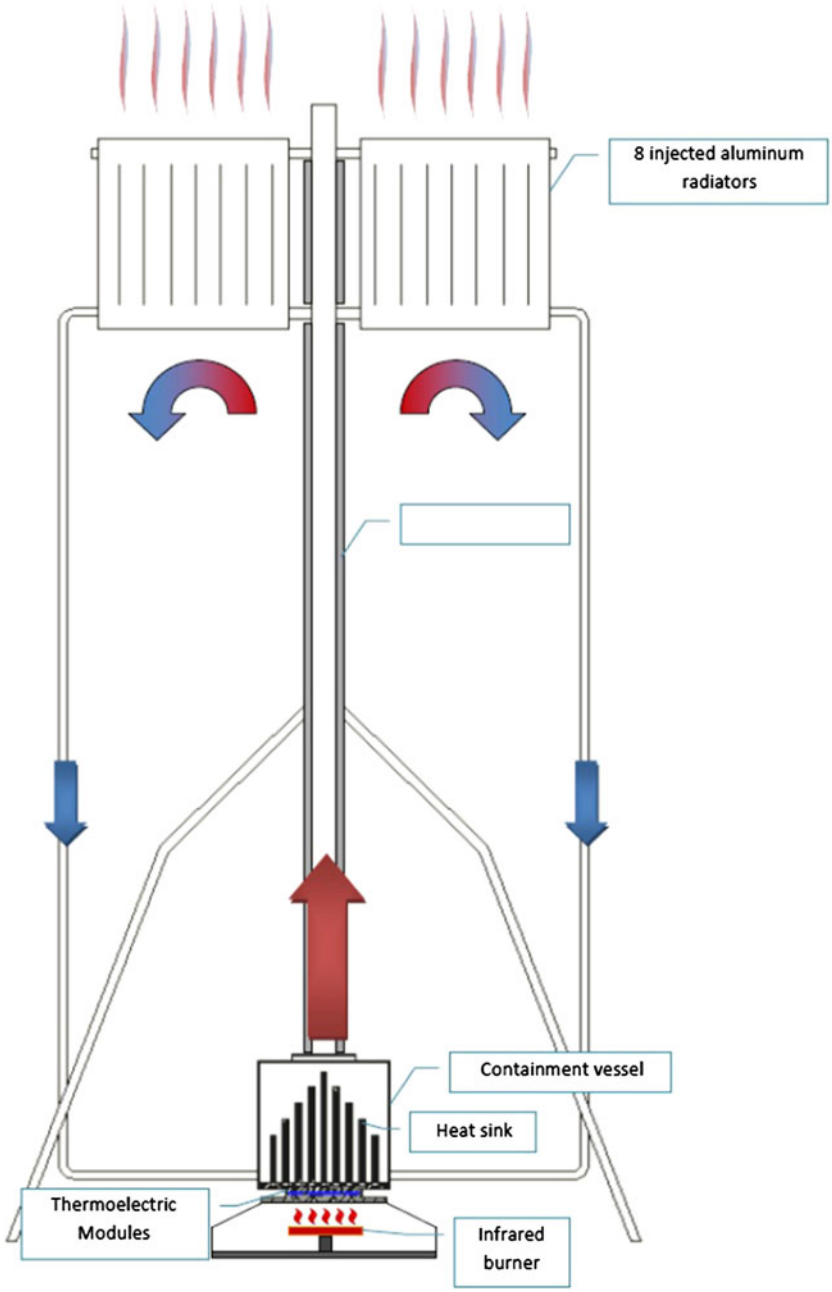

Fig. 2. General schematic of the prototype.

Author's personal copy

The temperatures of both legs (T_1, T_2) are determined by the thermal modeling according to the set of boundary conditions, i.e., the heating power and ambient temperature. The heating power transferred to the heat exchanger (P_h) is balanced by the mass flow (m'), heat capacity C_p, and the temperature drop according to its energy balance[9]:

$$P_h = m' C_p (T_1 - T_2). \quad (5)$$

Assuming (conservatively) that all tubes are adiabatic, this heating power must be balanced by the heat dissipated by the radiators (P_r) at ambient temperature, T_0. Every radiator is formed by six dissipative elements, each with the following curve which was experimentally fitted[10]:

$$P_r = 0.01391\ \Delta T_r^2 + 3.1586 \Delta T_r, \quad (6)$$

where ΔT_r is the average temperature drop between the radiator and environment, defined (following the adiabatic assumption) as $\Delta T_r = (T_1 + T_2)/2 - T_0 = T_m - T_0$. So, from the boundary conditions (T_0, $P_h = P_r$) the average ΔT_r is calculated from Eq. (6) considering all the (48) radiator elements. From here, the actual (T_1, T_2) values can be determined following an iterative procedure, according to the previous Eqs. (1–6), in which $T_1 = T_m + \varepsilon$ and $T_2 = T_m - \varepsilon$, where ε is initially an infinitesimal value that is incremented gradually until a balance of energy ($P_h = P_r$) is obtained. After that, the temperature of the TE cold side can be estimated by the thermal resistance of the aluminum–water node, R_{HE}. This R_{HE} value was estimated by using a one-dimensional thermal model for the finned dissipator[10] as $R_{HE} = 5.8 \times 10^{-3}$°C/W. Thus, for example, for a heating flux of 2500 W (estimated for 120 W of thermoelectric generation) a cold-side drop of 14°C is obtained.

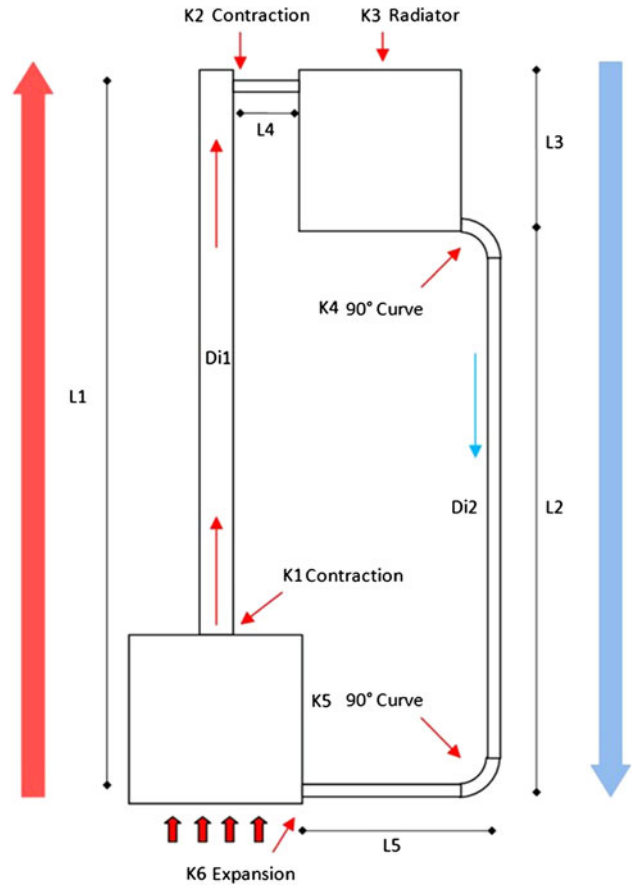

Fig. 3. Schematic of hydraulic loop model.

NUMERICAL RESULTS

This hydraulic and thermal modeling was numerically studied for different boundary conditions. Figure 4 summarizes the whole numerical procedure performed in the Simulink framework. In this way, all temperatures can be calculated, such as the water loop temperatures and both thermoelectric temperatures. Hence, the thermoelectric generation can be estimated from the thermopile temperature drop ΔT_{TE} by the following experimentally fitted equation[10]:

$$P = 5 \times 10^{-4} (\mathrm{W}/^{\circ}\mathrm{C}^2) \Delta T_{TE}^2. \quad (7)$$

Figure 5 summarizes the power generation calculated related to the heating power parameterized for T_0 = 0°C, 20°C, and 40°C, where the maximum power obtained is 150 W, 120 W, and 90 W, respectively. Here it is observed that T_0 has a noticeable effect on the thermogenerator performance, since the power generated can be almost doubled in winter conditions (0°C) in comparison with summer conditions (40°C). On the contrary, Global Thermoelectric's thermogenerator that does not have a heat controller cannot regulate its

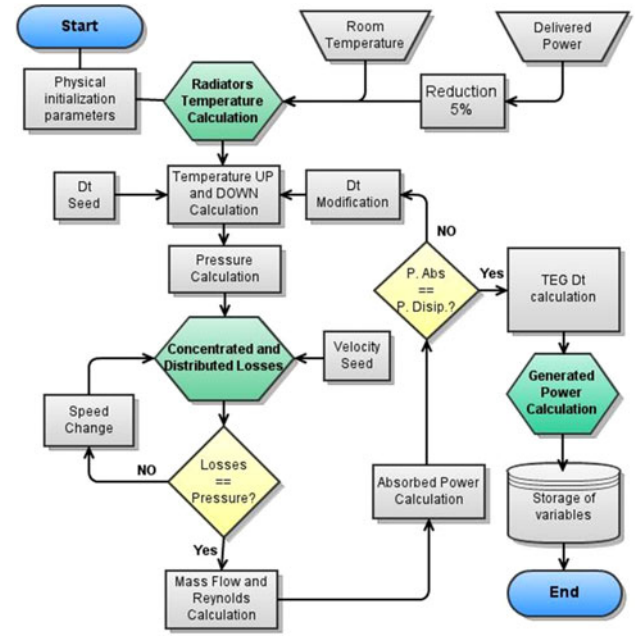

Fig. 4. Flowchart of the numerical calculation procedure.

Author's personal copy

heating power, so the burner must be set for the whole year according to the most demanding (summer) conditions. This trend justifies our choice for a microcontroller that regulates the instantaneous burner power at any time.

EXPERIMENTAL STUDY

The thermal–hydraulic modeling performed above was experimentally studied on the developed prototype. Figure 6 shows the whole prototype built and tested together with partial mounting views in Figs. 7–9. A complete description is given in a master's thesis,[10] including other features such as the very high-frequency (VHF) telecommunication system, an electronic switching-on system, and the mechanical and thermomechanical designs.

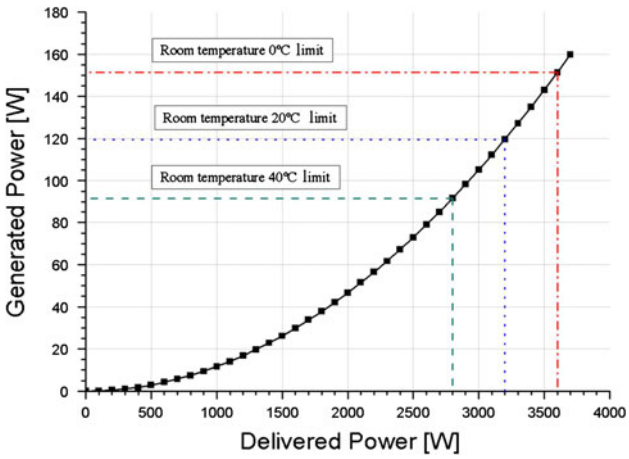

Fig. 5. Power generation versus heating power.

Fig. 6. Overall picture of prototype.

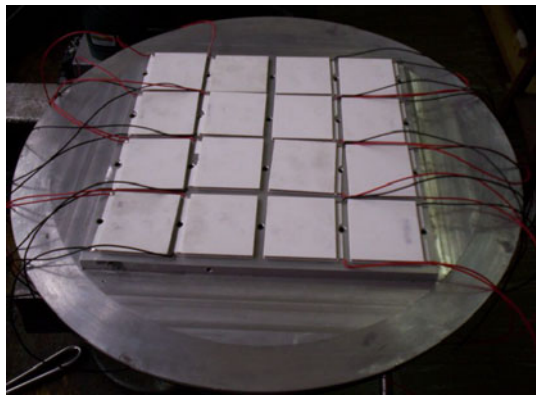

Fig. 7. Mounting view of the TE assembly mounted onto the dissipator plate (in inverted position).

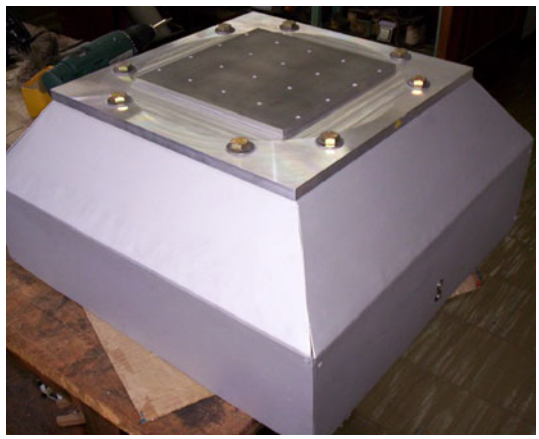

Fig. 8. Mounting view of the collector plate and the deflector shield of the burner.

Fig. 9. Mounting view of the water heat exchanger mounted onto the TE assembly.

Author's personal copy

Table I. Comparison between measured and model–predicted temperatures (T_0 = 20°C)

	Model	Test
TE generation (W)	78	79
Hot-side temperature (°C)	135	145
Cold-side temperature (°C)	50	53
Radiator temperature (°C)	35	33

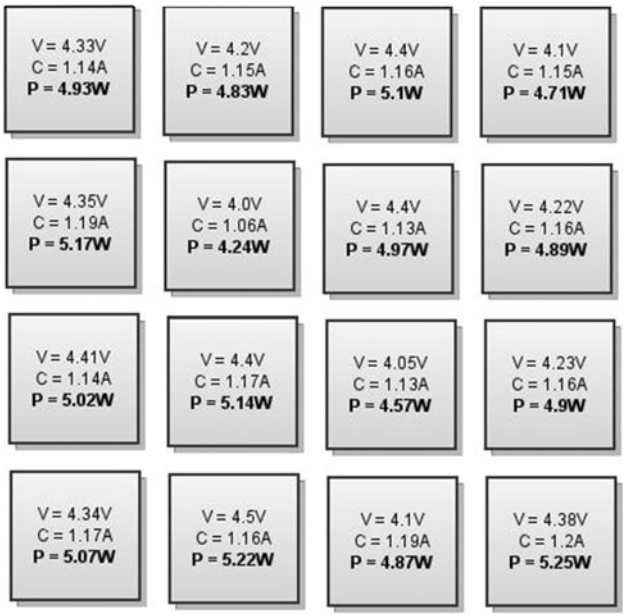

Fig. 10. Electrical measurements on TE modules for previous testing conditions.

Several experimental tests were performed, and it was observed that they qualitatively reproduced the steady-state conditions previously summarized in Fig. 5. All tests allowed us to validate this thermal model within a 15% error. Table I presents a comparison between the measured and model-predicted temperatures for a steady-state condition (generating 79 W) with T_0 = 20°C for which the electrical signals (voltage, current, and power generated) measured on every TE module are shown in Fig. 10. Here a very homogenized temperature is obtained. Considering the major concerns regarding the contact forces between the fragile ceramic TE modules and both aluminum plates, this picture reflects that a good thermomechanical design was achieved.

ANALYSIS OF COSTS

The cost breakdown of this 120-W prototype is presented in Table II. A specific total cost of about 55,000 USD/kW is calculated, slightly lower than the price of Global Thermoelectric's commercial equipment. In addition, it is observed that large mechanical systems represent around 50% of the total cost. Thus, a noticeable cost reduction can be expected for higher-power generators according to the well-known 2/3 power law for upscaling mechanical equipment. This assumption can be extended to other items with the single exception of the TE modules (18%), for which a constant specific cost is used. In this way and for the example of a 1 kW generator, a reduction of 42% is achieved, with costs of about 33,000 USD/kW (Table II). The high modularity of this design allows us to obtain a higher-power unit at competitive total cost.

Table II. Cost for the 120-W prototype and a larger (1 kW) one

	120-W Prototype		1 kW	
Item	Cost (USD)	%	Cost (USD)	%
Water radiators	1250	19	5100	16
TE modules	1200	18	10,000	31
Heat exchanger	1000	15	4100	13
Mechanical assembly	750	11	3000	9
Piping	500	7	2000	6
Mechanical structure	500	7	2000	6
Collecting plate	250	4	1000	3
Electronic board	300	4	1200	4
Telecommunication system	300	4	1200	4
Infrared burner	150	2	600	2
Pressurization	100	1	400	1
Solenoid valves	100	1	400	1
Miscellaneous	300	4	1200	4
Total (USD)	6700	100	32,600	100
Specific cost (USD/kW)	55,800		32,600	

CONCLUSIONS

In this paper an innovative design for a thermogenerator intended to work in unattended remote applications is presented. The main innovation relates to its successful cooling system, which allowed us to develop a prototype based on moderate-temperature BiTe thermoelectric modules that provide a low-cost modular technology suitable for upscaling. In this way, very competitive costs (about 33,000 USD/kW) could be obtained for larger (1 kW) units; this represents half the market price of present commercial generators.

On the other hand, the other added feature of remote-control and microcontrolled heating power allows this thermogenerator to maximize the power generated under any conditions, considering the noticeable effect of the ambient temperature observed on its performance. In addition, this feature is useful to guarantee safe operation (without TE overheating). This capability gives a technological advantage to the new technology related to the presented thermogenerators.

The thermal–hydraulic modeling performed has been demonstrated to be a useful tool for achieving

Author's personal copy

an optimized design, and the developed prototype and experimental tests performed have demonstrated the feasibility of this technology. Moreover, by using the new BiTe modules recently released onto the market that can withstand up to 320°C, costs can be significantly reduced, conferring this new technology a very favorable outlook.

REFERENCES

1. 8550 Thermoelectric Generator Operating Manual, 23658 Rev. 4, Global Thermoelectric (1992).
2. R. Nuwayhid and R. Hamade, *Renew. Energy* 30, 1101 (2005).
3. A. Killander and J. Bass, *International Conference on Thermoelectrics*, Pasadena, U.S., (1996).
4. D. Mastbergen, B. Willson and S. Joshi. Producing light from stoves using a thermoelectric generator, http://bioenergylists.org/stovesdoc/ethos/mastbergen/Mastbergen_ETHOS_2005.pdf. Accessed 21, December 2012.
5. L. Juanicó, F. Rinalde, E. Taglialavore and M. Molina, *International Conference on Thermoelectrics*, Aalborg, Denmark, (2012).
6. See web site of Tellurex, http://www.tellurex.com.
7. See web site of Thermonamic, http://www.thermonamic.com/.
8. F. White, *Fluid Mechanics*, 6th ed. (New York: McGraw-Hill, 2006).
9. F. Incropera. D. DeWitt, T. Bergman, and A. Lavinne. *Fundamentals of Heat and Mass Transfer*, 6th ed., (Wiley, New Jersey, 2007).
10. L. Juanicó, F. Rinalde, and E. Taglialavore, *Prototipos de Termogeneradores para Electrificación Aislada* (Spain: Ed. Académica Española Pub, 2012).